Journal of Basic & Applied Sciences, 2025, *21*, 88-100

Published by SET Publisher

Journal of Basic & Applied Sciences

ISSN (online): 1927-5129

Sensitivity Analysis of a Supersonic Airfoil's Optimal Design Using Taylor Series

Cheng Luo[1,*], Zhenxue Han[1] and Owen Luo[2]

[1]*Department of Mechanical and Aerospace Engineering, University of Texas, Arlington, TX, USA 76019, USA*

[2]*Winston Churchill High School, 11300 Gainsborough Road, Potomac, MD 20854, USA*

Article Info:

Keywords:
Taylor series,
Optimal design,
Factorial design,
Sensitivity analysis,
Finite-difference method.

Timeline:
Received: January 29, 2025
Accepted: February 22, 2025
Published: March 25, 2025

Citation: Luo C, Han Z, Luo O. Sensitivity Analysis of a Supersonic Airfoil's Optimal Design Using Taylor Series. J Basic Appl Sci 2025; 21: 88-100.

DOI: https://doi.org/10.29169/1927-5129.2025.21.10

*Corresponding Author
E-mail: chengluo@uta.edu

Abstract:

In this study, we conducted a sensitivity analysis to determine the optimal design of a supersonic airfoil. The design includes four independent variables: angle of attack, thickness of the upper surface, and the locations of the upper and lower surfaces' maximum thicknesses. The output is the maximum lift-to-wave drag ratio. First, we used a first-order Taylor approximation to analyze the impact of each design variable on the output. The first three variables have similar effects, while the fourth has less influence. Next, we applied a second-order Taylor approximation to further explore how each variable affects the output and the response function near the optimal design point. The results show that small variations in the design variables lead to minor changes in airfoil performance. We also identified the variable ranges around this point that satisfy the constraints through numerical calculations. Finally, we compared our approach with factorial design, a common sensitivity analysis method, and found that Taylor approximations offer a more detailed theoretical explanation of the results.

1. INTRODUCTION

In practice, the dimensions of a manufactured structure may deviate from the designed specifications due to manufacturing errors. For safety reasons, it is crucial to understand how these variations impact the structure's performance. Additionally, when a design is influenced by numerous factors, it becomes essential to identify the most critical ones. Without this, conducting experiments or simulations to identify the necessary parameters for establishing a predictive model of system behavior under varying conditions can become overly complex and time-consuming. Therefore, sensitivity analysis plays a key role in engineering design. It helps to assess how changes in input parameters impact the system's output and identifies the most significant factors influencing performance.

Factorial design is widely used for sensitivity analysis in various engineering problems [1,2], such as the designs of aerodynamic off-takes [3-6] and ducts [6], the optimization of plasma etching processes in semiconductor manufacturing [2], and the 3D printing of composite structures [7] and polymeric auxetic structures [8]. This approach involves systematically varying multiple input variables simultaneously to assess their individual and combined effects on the output. As noted in [9], this method was already used in the 19th century for fertilizer trials. It was developed from the statistical perspective, aimed at finding the effects of various factors and their interactions on the output [10]. For this purpose, a set of experiments was designed, and the combinations of experimental results were analyzed to determine these effects [10-12,1,2].

The 2^k and 3^k factorial designs are frequently used to construct first- and second-order models [10-12,1,2], where k denotes the number of input parameters in a model. In the 2^k factorial design, the output is assumed to depend linearly on each factor and their interactions. The minimum and maximum values of each factor are considered. If there are two factors, their minimum and maximum values create 2^2=4 possible combinations, requiring 4 tests. Based on the assumption of linearity, the results are used to determine which factor or interaction has significant effect on the output. When the output exhibits a nonlinear relationship with the factors, a nonlinear model should be developed, with the simplest being a second-order model. In this case, using the 3^k factorial design, the minimum, mean, and maximum values of each factor are considered, resulting in 3^k possible combinations. Accordingly, 3^k experiments are conducted. The coefficients of the second-order model are then determined using the experimental data and regression techniques, such as least-squares estimation.

Airfoils are well known to significantly impact the performance of aerodynamic bodies, such as aircraft [13-16], helicopters [17,18], micro-air vehicles [19,20], propellers [21,22], and wind turbines [23,24]. Fluctuations of angle of attack and manufacture defects could result in a dramatic change of the aerodynamic performance of an aircraft. Factorial designs can be applied to assess the robustness of airfoil designs. Recently, we determined the optimal design of a supersonic aircraft's airfoil [25]. In this study, we aim to conduct a sensitivity analysis of this design to examine how small variations affect the aerodynamic performance of the corresponding airfoil. Rather than directly applying the factorial design method, we utilize first- and second-order approximations of the objective function derived from Taylor expansion. We also explore their relationships with the 2^k and 3^k factorial designs.

This paper is outlined as follows. Section 2 presents the development of the first- and second-order models based on Taylor expansion and factorial designs. Section 3 introduces the optimal design problem. Section 4 discusses the sensitivity analysis of the design, and Section 5 provides a summary and conclusion of the study.

2. PROBLEM DEFINITION

Consider an airfoil for a supersonic aircraft (Figure **1**). The airfoil features a thin section formed of either angled panels or opposed arcs with sharp leading and trailing edges. A rectangular coordinate system is established, with the *x*-axis aligned along the chord of the airfoil and the *y*-axis perpendicular to it. The origin is located at the leading edge of the airfoil. Let t_u and t_l represent the maximum thicknesses of the upper and lower surfaces, respectively. The total thickness t of the airfoil is related to t_u and t_l by $t= t_u+t_l$. Let c_l denote the lift coefficient, and c_d represent the wave drag coefficient. Use α to denote the angle of attack, which is the angle between the chord of the airfoil and the incoming airflow. The airfoil's dimensions are nondimensionalized with respect to the chord length, which is normalized to 1. In [25], an optimal design for the supersonic airfoil was derived based on the following six constraints:

i. t =0.1;

ii. $c_l \geq 0.3$;

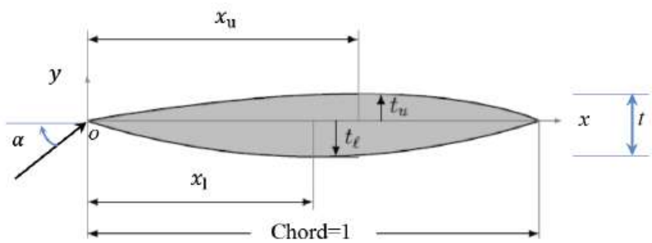

Figure 1: Sketch of a supersonic airfoil.

iii. $|c_m| \leq 0.1$

iv. $1/3 \leq x_u \leq 2/3$;

v. $1/3 \leq x_l \leq 2/3$; and

vi. $0^o \leq \alpha \leq 10^o$.

The design Mach number is 3.0, meaning the aircraft's speed is three times the speed of sound. There are four design variables: α, t_u, x_u, and x_l. The objective function is

$$f(\alpha, t_u, x_u, x_l) = \frac{c_l}{c_d}. \tag{1}$$

The goal is to find a set of these design variables that maximizes $\frac{c_l}{c_d}$, while ensuring that all six constraints are satisfied. Three algorithms have been used in [25] to determine an optimal design. The first algorithm was developed to numerically calculate c_l and c_d using shock/expansion wave theory [26]. The second and third algorithms-Exhaustive search [27] and Basin-Hopping [28,29]-were then applied to solve the corresponding optimization problem. The Basin-Hopping provided the best optimal design with high efficiency. The optimal design resulted in a $\frac{c_l}{c_d}$ value of 3.312, with the following design parameters: α=9.82^o, t_u=0.024, x_u=0.667, and x_l =0.500.

Due to manufacturing constraints, the geometrical dimensions of the fabricated airfoil, such as x_u, might have errors of a few percent. This raises the question: how do small variations in the design variables affect the $\frac{c_l}{c_d}$ ratio in practice? To answer this question, a sensitivity analysis is conducted here with respect to the function $f(\alpha, t_u, x_u, x_l)$. As there is no explicit expression for this response function in the context of this design problem, the analysis will reply on the numerical evaluation of the function at points near the critical point of the optimal design. To optimize computational effort, the number of evaluation points will be limited.

3. TAYLOR SERIES AND 2^K AND 3^K FACTORIAL DESIGNS

3.1. First-Order Models

The Taylor series provides a way to approximate the objective function near the critical point of the optimal design, utilizing the function values at and near this point, along with its derivatives at the critical point. It is first used here to determine the first- and second-order approximations of the objective function.

Consider a real function $f(x_1, \ldots, x_k)$, where x_1 through x_k represent its k independent variables. Assume that the function is at least twice differentiable. Its first-order approximation in a small neighborhood around a point *p*, with coordinates $(x_{10}, \ldots, x_{k0})$, can be derived by keeping the first two terms of its Taylor series at *p*, as given below:

$$f(x_1, \ldots, x_k) = f(x_{10}, \ldots, x_{k0}) + \sum_{i=1}^{k} \frac{\partial f(x_{10}, \ldots, x_{k0})}{\partial x_i}(x_i - x_{i0}) + O(h^2), \tag{2}$$

where $\frac{\partial f(x_{10}, \ldots, x_{k0})}{\partial x_i}$ denotes the partial derivative of *f* with respect to x_i at the point *p*, *h* represents the maximum value of $|x_1 - x_{10}|$, …, $|x_k - x_{k0}|$, and $O(h^2)$ represents the higher-order terms neglected in Eq. (2), with an order of magnitude of h^2.

To better understand Eq. (1) and its application to evaluate the effect of each independent variable, let's consider a simple case, where *f* has only two independent variables, x_1 and x_2. For this case, Eq. (2) becomes

$$f(x_1, x_2) = f(x_{10}, x_{20}) + \frac{\partial f(x_{10}, x_{20})}{\partial x_1}(x_1 - x_{10}) + \frac{\partial f(x_{10}, x_{20})}{\partial x_2}(x_2 - x_{20}) + O(h^2). \tag{3}$$

According to the central difference method [30], which is one of the finite-difference methods to calculate the first derivatives numerically [30,31], the two partial derivatives in Eq. (3) can be expressed in terms of the function values at four points surrounding *p*. The four points chosen here have the coordinates $(x_{10} + h_1, x_{20})$, $(x_{10} - h_1, x_{20})$, $(x_{10}, x_{20} + h_2)$, and $(x_{10}, x_{20} - h_2)$, where h_1 and h_2 are positive values of the same order of magnitude as *h* (Figure **2**). Accordingly,

$$\frac{\partial f(x_{10}, x_{20})}{\partial x_1} = \frac{f(x_{10} + h_1, x_{20}) - f(x_{10} - h_1, x_{20})}{2h_1} + O(h^2), \tag{4}$$

$$\frac{\partial f(x_{10},x_{20})}{\partial x_2} = \frac{f(x_{10}, x_{20}+h_2)-f(x_{10}, x_{20}-h_2)}{2h_2} + O(h^2). \quad (5)$$

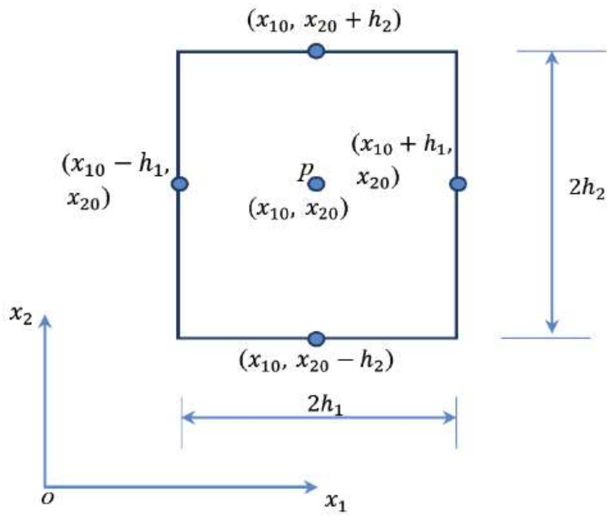

Figure 2: Five points where the function values need to be known to determine the first-order approximation of a two-variable function around the point *p*, using Taylor expansion and central difference method.

Substituting Eqs. (4) and (5) into Eq. (3) yields

$$f(x_1,x_2) = f(x_{10},x_{20}) + \frac{f(x_{10}+h_1,x_{20})-f(x_{10}-h_1,x_{20})}{2h_1}(x_1 - x_{10}) + \frac{f(x_{10}, x_{20}+h_2)-f(x_{10}, x_{20}-h_2)}{2h_2}(x_2 - x_{20}) + O(h^2). \quad (6)$$

According to Eq. (6), once the function values at the four points $(x_{10}+h_1, x_{20})$, $(x_{10}-h_1, x_{20})$, $(x_{10}, x_{20}+h_2)$, and $(x_{10}, x_{20}-h_2)$ are known (Figure **2**), the expression of $f(x_1,x_2)$ is fully determined.

Next, let's consider the effects of the variations in x_{10} and x_{20} on the change in function value. Assume that due to, for instance, manufacturing errors, the values of x_{10} and x_{20} change to x_1 and x_2, respectively. Let Δx_1 and Δx_2 denote their respective changes. Set $\Delta f(\Delta x_1,\Delta x_2)$ to be the corresponding change in the function value. Then,

$$\Delta x_1 = x_1 - x_{10}, \quad (7)$$

$$\Delta x_2 = x_2 - x_{20}, \quad (8)$$

$$\Delta f(\Delta x_1,\Delta x_2) = f(x_1,x_2) - f(x_{10},x_{20}). \quad (9)$$

With the aid of Eqs. (7)-(9), it follows from Eq. (6) that

$$\Delta f(\Delta x_1,\Delta x_2) = \frac{f(x_{10}+h_1,x_{20})-f(x_{10}-h_1,x_{20})}{2h_1}\Delta x_1 + \frac{f(x_{10}, x_{20}+h_2)-f(x_{10}, x_{20}-h_2)}{2h_2}\Delta x_2 + O(h^2). \quad (10)$$

It can be observed from Eq. (10) that the first and second terms on the right-hand side of this equation are associated with the changes of the function value that are induced by Δx_1 and Δx_2, respectively. If there is only a variation in x_{10}, the induced change in the function value, denoted as Δf_1, is

$$\Delta f_1(\Delta x_1) = \frac{f(x_{10}+h_1,x_{20})-f(x_{10}-h_1,x_{20})}{2h_1}\Delta x_1 + O(h^2). \quad (11)$$

Similarly, if there is only a variation in x_{20}, the induced change in the function value, denoted as Δf_2, is

$$\Delta f_2(\Delta x_2) = \frac{f(x_{10}, x_{20}+h_2)-f(x_{10}, x_{20}-h_2)}{2h_2}\Delta x_2 + O(h^2). \quad (12)$$

When variations exist in both x_{10} and x_{20}, Eq. (10) should be applied to estimate the change in the function value. If $\Delta f_1(\Delta x_1)$ is much larger than $\Delta f_2(\Delta x_2)$, then Δx_1 has significantly greater influence on $\Delta f(\Delta x_1,\Delta x_2)$. Conversely, if $\Delta f_1(\Delta x_1)$ is much smaller than $\Delta f_2(\Delta x_2)$, then Δx_2 has the dominating effect on $\Delta f(\Delta x_1,\Delta x_2)$.

For the general case with *k* independent variables, following the same reasoning, the change in function value is related to the variations of the independent variables by:

$$\Delta f(\Delta x_1, \dots, \Delta x_k) = \sum_{i=1}^{k} \frac{f(x_{10},\dots,x_{i0}+h_i,x_{k0})-f(x_{10},\dots,x_{i0}-h_i,x_{k0})}{2h_i}\Delta x_i + O(h^2). \quad (13)$$

As seen from this equation, the function values at 2*k*+1 points, including the point *p*, must be known.

Using the forward difference method [30], which is another finite-difference method to calculate the first derivatives numerically [30,31], the two partial derivatives in Eq. (3) can also be expressed in terms of the function values at two points around *p*, with the coordinates $(x_{10}+h_1, x_{20})$ and $(x_{10}, x_{20}+h_2)$ (Figure **3**). The corresponding expressions are:

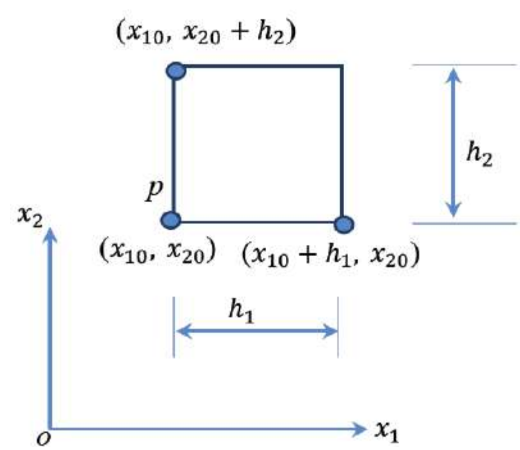

Figure 3: Three points where the function values need to be known to determine the first-order approximation of a two-variable function around the point *p*, using Taylor expansion and the forward difference method.

$$\frac{\partial f(x_{10},x_{20})}{\partial x_1} = \frac{f(x_{10}+h_1,x_{20})-f(x_{10},x_{20})}{h_1} + O(h), \quad (14)$$

$$\frac{\partial f(x_{10},x_{20})}{\partial x_2} = \frac{f(x_{10},x_{20}+h_2)-f(x_{10},x_{20})}{h_2} + O(h). \quad (15)$$

As shown in Eqs. (14) and (15), the use of the forward difference method to determine a partial derivative introduces an error of $O(h)$. Therefore, this method is less accurate than the central difference method in estimating the derivative. However, it can be shown that after Eqs. (14) and (15) are submitted into Eq. (2), the resulting equation still includes an error term of $O(h^2)$, as given below:

$$f(x_1,x_2) = f(x_{10},x_{20}) + \frac{f(x_{10}+h_1,x_{20})-f(x_{10},x_{20})}{h_1}(x_1 - x_{10}) + \frac{f(x_{10},x_{20}+h_2)-f(x_{10},x_{20})}{h_2}(x_2 - x_{20}) + O(h^2). \quad (16)$$

According to Eq. (16), once the function values at the three points (x_{10}, x_{20}), $(x_{10}+h_1, x_{20})$, and $(x_{10}, x_{20}+h_2)$ are known (Figure **3**), the expression of $f(x_1,x_2)$ is determined. For this case, as done when the partial derivatives are calculated using the central difference method,

$$\Delta f_1(\Delta x_1) = \frac{f(x_{10}+h_1,x_{20})-f(x_{10},x_{20})}{h_1}\Delta x_1 + O(h^2), \quad (17)$$

$$\Delta f_2(\Delta x_2) = \frac{f(x_{10},x_{20}+h_2)-f(x_{10},x_{20})}{h_2}\Delta x_2 + O(h^2). \quad (18)$$

$$\Delta f(\Delta x_1,\Delta x_2) = \frac{f(x_{10}+h_1,x_{20})-f(x_{10},x_{20})}{h_1}\Delta x_1 + \frac{f(x_{10},x_{20}+h_2)-f(x_{10},x_{20})}{h_2}\Delta x_2 + O(h^2). \quad (19)$$

For the general case with *k* independent variables, following the same reasoning, the change in function value is related to the variations in the independent variables by:

$$\Delta f(\Delta x_1,\ldots,\Delta x_k) = \sum_{i=1}^{k}\frac{f(x_{10},\ldots,x_{i0}+h_i,x_{k0})-f(x_{10},\ldots,x_{i0},x_{k0})}{h_i}\Delta x_i + O(h^2). \quad (20)$$

As observed from this equation, the function values at *k*+1 points, including the point *p*, should be known to determine Δf.

Next, let's determine the effects of Δx_1 and Δx_2 on $\Delta f(\Delta x_1,\Delta x_2)$ using a 2^k factor design, where 2 means that two levels of values (i.e., two different values) are considered for each independent variable in the design. Consider the simple case again. As the function has two independent variables, *k*=2. Since 2^2=4, the function values should be determined by experiments or simulation at four points in the design variable space. These points are: (x_{10}, x_{20}), $(x_{10}+\Delta x_1, x_{20})$, $(x_{10}, x_{20}+\Delta x_2)$, and $(x_{10}+\Delta x_1\ \ x_{20}+\Delta x_2)$ (Figure **4**). The influence of Δx_1 and Δx_2 on Δf is determined by comparing the corresponding main effects. The main effect is defined as the change in the function produced by a change in the level of an independent variable, averaged over the levels of the other variable(s). Let E_1 and E_2 denote the main effects of x_1 and x_2, respectively. Then,

$$E_1 = \frac{f(x_{10}+\Delta x_1,x_{20})+f(x_{10}+\Delta x_1,\ x_{20}+\Delta x_2)-f(x_{10},\ x_{20})-f(x_{10},\ x_{20}+\Delta x_2)}{2}, \quad (21)$$

$$E_2 = \frac{f(x_{10},x_{20}+\Delta x_2)+f(x_{10}+\Delta x_1,\ x_{20}+\Delta x_2)-f(x_{10},x_{20})-f(x_{10}+\Delta x_1,\ x_{20})}{2}. \quad (22)$$

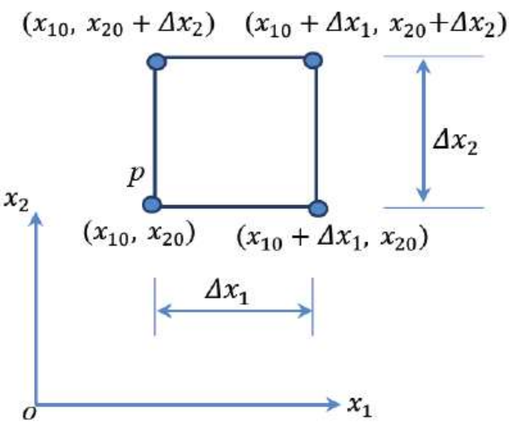

Figure 4: Four points where the function values need to be known in order to estimate the main effects around the point *p* and to construct a first-order model using a 2^2 factorial design.

They can be re-written as:

$$E_1 = \frac{[f(x_{10}+\Delta x_1,x_{20})-f(x_{10},\ x_{20})]+[f(x_{10}+\Delta x_1,\ x_{20}+\Delta x_2)-f(x_{10},\ x_{20}+\Delta x_2)]}{2}, \quad (23)$$

$$E_2 = \frac{[f(x_{10},x_{20}+\Delta x_2)-f(x_{10},x_{20})]+[f(x_{10}+\Delta x_1,\ x_{20}+\Delta x_2)-f(x_{10}+\Delta x_1,\ x_{20})]}{2}. \quad (24)$$

According to the forward difference method, the items inside each pair of square brackets in Eqs. (23) and (24) are related to the corresponding partial derivatives as follows:

$$f(x_{10}+\Delta x_1,\ x_{20}) - f(x_{10},\ x_{20}) = \frac{\partial f(x_{10},x_{20})}{\partial x_1}\Delta x_1 + O(\Delta x_1), \quad (25)$$

$$f(x_{10}+\Delta x_1,\ x_{20}+\Delta x_2) - f(x_{10},\ x_{20}+\Delta x_2) = \frac{\partial f(x_{10},\ x_{20}+\Delta x_2)}{\partial x_1}\Delta x_1 + O(\Delta x_1), \quad (26)$$

$$f(x_{10},\ x_{20}+\Delta x_2)-f(x_{10},\ x_{20})=\frac{\partial f(x_{10},x_{20})}{\partial x_2}\Delta x_2+O(\Delta x_2), \tag{27}$$

$$f(x_{10}+\Delta x_1,\ x_{20}+\Delta x_2)-f(x_{10}+\Delta x_1,\ \ x_{20})=\frac{\partial f(x_{10}+\Delta x_1,\ x_{20})}{\partial x_2}\Delta x_2+O(\Delta x_2). \tag{28}$$

In a 2^k factor design, it is assumed that the function f depends linearly on its independent variables. This assumption implies that the partial derivative of f with respect to each independent variable is a constant. That is, it does not vary with the values of other variables. As such,

$$\frac{\partial f(x_{10},\ x_{20}+\Delta x_2)}{\partial x_1}=\frac{\partial f(x_{10},\ x_{20})}{\partial x_1}, \tag{29}$$

$$\frac{\partial f(x_{10}+\Delta x_1,\ x_{20})}{\partial x_2}=\frac{\partial f(x_{10},x_{20})}{\partial x_2}. \tag{30}$$

Furthermore, the linearity assumption ensures that there is no error when using the forward or central difference method to estimate the derivatives. Therefore, in Eqs. (25)-(28), all error terms are zero. With the aid of Eqs. (25)-(30), it follows from Eqs. (23) and (24) that

$$E_1=\frac{\partial f(x_{10},x_{20})}{\partial x_1}\Delta x_1, \tag{31}$$

$$E_2=\frac{\partial f(x_{10},x_{20})}{\partial x_2}\Delta x_2. \tag{32}$$

Comparing Eqs. (31) and (32) with Eq. (3), it becomes evident that E_1 and E_2 correspond to the second and third terms of Eq. (3). Accordingly, using E_1 and E_2 to determine the effect of each variable is effectively the same as applying the first-order Taylor approximation for this purpose.

With the assistance of Eqs. (25) and (27), Eqs. (31) and (32) can also be written as

$$E_1=f(x_{10}+\Delta x_1,\ x_{20})-f(x_{10},\ \ x_{20}), \tag{33}$$

$$E_2=f(x_{10},\ x_{20}+\Delta x_2)-f(x_{10},\ x_{20}). \tag{34}$$

These equations provide specific expressions of E_1 and E_2 in terms of the function values at three points. In other words, when the function values linearly depend on the two independent variables, respectively, only the function values at three points need to be determined, rather than four. With four points required in a 2^2 factorial design, partial derivatives at two different points can be found, and their average is used as the value for the partial derivative in Eq. (31) or (32). This approach reduces the risk of inaccuracies caused by experimental errors at a single point when calculating the derivative.

For the general case with k independent variables, following the same reasoning, the main effect of each independent variable is:

$$E_i=f(x_{10},\dots x_{i0}+\Delta x_i,\dots,\ x_{k0})-f(x_{10},\dots x_{i0},\dots,\ x_{k0}). \tag{35}$$

As seen from this equation, the function values at k+1 points, including the point p, should be known to determine all main effects.

Furthermore, when the values of Δx_1 and Δx_2 differ from those tested in the experiments, Eqs. (33) and (34) cannot be used to accurately assess the effects of the new Δx_1 and Δx_2 on Δf. These equations can only be used to estimate the effects. To obtain a more accurate estimation of these effects, new tests should be conducted to determine the values of $f(x_{10}+\Delta x_1,\ x_{20})$ and $f(x_{10},\ x_{20}+\Delta x_2)$ for new Δx_1 and Δx_2. These values are essential for calculating the corresponding E_1 and E_2 according to Eqs. (33) and (34). On the other hand, if Eqs. (11) and (12) are used to evaluate the effects, once the values of the function at the four points are determined, the effects of the new Δx_1 and Δx_2 on Δf can be determined using Eqs. (11) and (12), without the need for additional tests.

In the 2^k factorial design, the first-order model with k independent variables has the following form [11,2]:

$$f(x_1,\dots,x_k)=a+\sum_{i=1}^{k}b_i\,x_i+\sum_{i=1}^{k}\sum_{j>i}^{k}C_{ij}\,x_ix_j, \tag{36}$$

where a, b_i and C_{ij} represent the coefficients. These coefficients are determined using the pre-established experimental or numerical datapoints and regression techniques [11,2]. For the simple case considered above,

$$f(x_1,x_2)=a+b_1x_1+b_2x_2+c_{12}x_1x_2. \tag{37}$$

A comparison of Eqs. (16) and (37) reveals that, although the first-order model in the factorial design includes a term involving x_1x_2, the first-order model derived from Taylor expansion does not involve such interaction terms. If the effect of x_1x_2 needs to be considered, it can be evaluated using a second-order model, which includes this interaction term. Additionally, the coefficients in Eq. (16) have well-defined mathematical meanings. In contrast, the coefficients in Eq. (37) are determined by the best data fit using the least-squares principle, and their exact mathematical interpretations remain unclear.

In summary, three key equations (i.e., Eqs. (13), (20), and (35)) have been derived to evaluate the effects of input parameters on the changes in function values, assuming that the function does not depend on the interactions between these parameters. All of these equations can be derived from the first-order Taylor approximation of the response function (i.e., Eq. (2)). However, they differed in the ways to calculate the partial derivatives numerically (as summarized in Table **1**). In practical applications, such as the optimal design of a supersonic airfoil, the response function is typically

Table 1: Comparison of Methods used for Deriving First- and Second-Order Models

Model	First-order Model Using Taylor Series and Central Difference Method	First-order Model Using Taylor Series and Forward Difference Method	First-order Model Using 2^k Factorial Design	Second-order Model Using Taylor Series, Central Difference and Finite-difference Methods	Second-order Model Using 3^k Factorial Design
Methods to build model	Tayler expansion, and central difference (for calculating first derivatives)	Tayler expansion, and forward difference (for calculating first derivatives)	2^k Factorial design, and first-order regression method (for finding coefficients)	Tayler expansion, central difference (for calculating first derivatives), and finite-difference (for calculating second derivatives)	3^k Factorial design, and second-order regression method (for finding coefficients)
No. of datapoints needed	$2k+1$	$k+1$	2^k	$2k^2+1$	3^k
Equations used to estimate the variable effects or the behavior of the function.	Eq. (13)	Eq. (20)	Eq. (35)	Eq. (38)	Eq. (46)
Degree of errors	$O(h^2)$ for calculating first derivatives.	$O(h)$ for calculating first derivatives.	$O(h)$ for calculating main effects.	$O(h^2)$ for calculating first and second derivatives.	N/A

non-linear, the first-order approximation often introduces significant errors. Specifically, the error term in Eq. (13), where the partial derivatives were computed using the central difference method, has an error order of h^2, which is an order of magnitude lower than those of the other two approaches, for which the partial derivatives were calculated using the forward difference method. Therefore, Eq. (13) will be employed here for the sensitivity analysis of our optimal design problem.

3.2. Second-order Models

In case where the function value does not linearly depend on the input variables, a second-order model may be used to approximate the function. The second-order approximation of $f(x_1, \dots, x_k)$ in the neighborhood of the point *p* is derived by retaining the first three terms of its Taylor expansion at *p*, as given below:

$$f(x_1,\dots,x_k) = f(x_{10},\dots,x_{k0}) + \sum_{i=1}^{k} \frac{\partial f(x_{10},\dots,x_{k0})}{\partial x_i}(x_i - x_{i0}) + 0.5\sum_{m=1}^{k}\sum_{n=1}^{k} \frac{\partial^2 f(x_{10},\dots,x_{k0})}{\partial x_m \partial x_n} x_m x_n + O(h^3), \quad (38)$$

where

$$\frac{\partial^2 f(x_{10},\dots,x_{k0})}{\partial x_m \partial x_n} = \frac{\partial^2 f(x_{10},\dots,x_{k0})}{\partial x_n \partial x_m}. \quad (39)$$

In contrast to the first-order approximation, the second-order approximation includes second-order partial derivatives of the function. The truncation error for the second-order approximation is of the order h^3. These second derivatives can be numerically calculated using finite-difference methods [30,31], as outlined below:

$$\frac{\partial^2 f(x_{10},\dots,x_{k0})}{\partial x_i^2} = \frac{f(x_{10},\dots,x_{i0}+h_i,\dots,x_{20}) + f(x_{10},\dots,x_{i0}-h_i,\dots,x_{20}) - 2f(x_{10},\dots,x_{i0},\dots,x_{k0})}{h_i^2} + O(h^2), \quad (40)$$

$$\frac{\partial^2 f(x_{10},\dots,x_{k0})}{\partial x_j \partial x_l} = \frac{\begin{matrix} f(x_{10},\dots,x_{j0}+h_j,\dots,x_{l0}+h_l,\dots,x_{20}) + f(x_{10},\dots,x_{j0}-h_j,\dots,x_{l0}-h_l,\dots,x_{k0}) \\ - f(x_{10},\dots,x_{j0}-h_j,\dots,x_{l0}+h_l,\dots,x_{20}) - f(x_{10},\dots,x_{j0}+h_j,\dots,x_{l0}-h_l,\dots,x_{k0}) \end{matrix}}{4h_j h_l} + O(h^2), \quad (41)$$

where both *j* and *l* range from 1 to *k* with the condition that $j \neq l$.

As observed from Eqs. (40) and (41), the second partial derivative of the function with respect to the same variable is determined using the function values at *p* and two points surrounding *p*. In contrast, the second partial derivative with respect to two different variables is calculated using the function values at four points around *p*. To obtain this second-order approximation, the function values at $2k^2+1$ points, which include *p*, must be known.

When the function has only two independent variables, it follows from Eqs. (38)-(41) that

$$f(x_1,x_2) = f(x_{10},x_{20}) + \frac{\partial f(x_{10},x_{20})}{\partial x_1}(x_1 - x_{10}) + \frac{\partial f(x_{10},x_{20})}{\partial x_2}(x_2 - x_{20}) + 0.5\left[\frac{\partial^2 f(x_{10},x_{20})}{\partial x_1^2} + \frac{\partial^2 f(x_{10},x_{20})}{\partial x_2^2} + 2\frac{\partial^2 f(x_{10},x_{20})}{\partial x_1 \partial x_2}\right] + O(h^3). \quad (42)$$

where

$$\frac{\partial^2 f(x_{10},x_{20})}{\partial x_1{}^2} = \frac{f(x_{10}+h_1, x_{20})+f(x_{10}-h_1,\ x_{20})-2f(x_{10}, x_{20})}{h_1{}^2} + O(h^2), \tag{43}$$

$$\frac{\partial^2 f(x_{10},x_{20})}{\partial x_2{}^2} = \frac{f(x_{10},\ x_{20}+h_2)+f(x_{10}, x_{20}-h_2)-2f(x_{10}, x_{20})}{h_2{}^2} + O(h^2), \tag{44}$$

$$\frac{\partial^2 f(x_{10},x_{20})}{\partial x_1 \partial x_2} = \frac{f(x_{10}+h_1, x_{20}+h_2)+f(x_{10}-h_1,\ x_{20}-h_2)-f(x_{10}-h_1,\ x_{20}+h_2)-f(x_{10}+h_1,\ x_{20}-h_2)}{4h_1h_2} + O(h^2). \tag{45}$$

For this case, where k=2, to determine the expression of f using Eq. (42), the function values should be known at nine points (Figure **5**). The function values at five of these points are used to specify the first three terms of Eq. (42). The function values at the additional four points are employed to determine the remaining terms, which correspond to the extra terms present in the second-order model compared to the first-order model (Figure **5**).

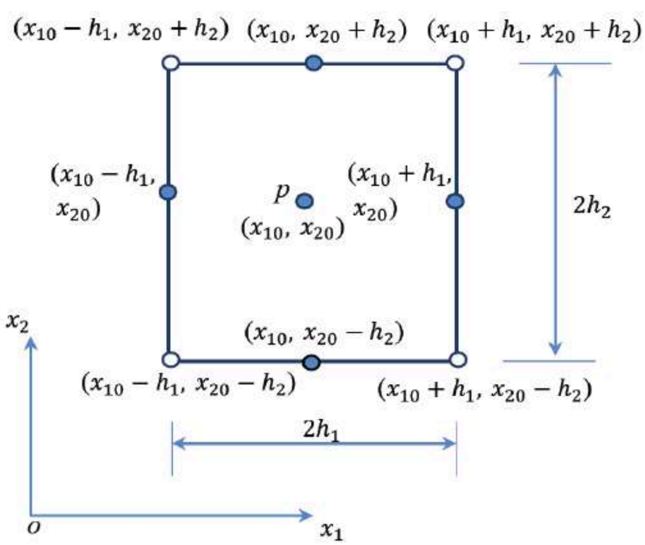

Figure 5: Nine points where the function values need to be known to determine the second-order approximation of a two-variable function around the point p using Taylor expansion. The five solid dots represent the points for the first-order approximation, and the four hollow dots denote the additional points needed for the second-order approximation.

The second-order model in factorial design is a second-order regression model with the following format [11,2]:

$$f(x_1, \dots, x_k) = a + \sum_{i=1}^{k} b_i\, x_i + \sum_{i=1}^{k} C_{ii}\, x_i{}^2 + \sum_{i=1}^{k}\sum_{j>i}^{k} C_{ij}\, x_i x_j. \tag{46}$$

This model includes $0.5k^2 + 1.5k + 1$coefficients, which are determined using regression techniques based on experimental or simulated datapoints. In the 3^k factorial design, the function values should be known at 3^k points, whereas for the second-order Taylor approximation, the function values should be known at $2k^2$+1 points (Table **1**). In the case where the function has only two independent variables, the function values need to be known at nine points to perform the factorial design. These nine points should be evenly distributed in the design variable space. For the simple case, the nine points shown in Figure **5** can be chosen to determine the coefficients in the second-order model of the factorial design.

In this study, since the second-order model, developed using Taylor expansion, has an explicit expression, its theoretical relationship Eq. (38), along with Eqs. (40) and (41), will be used to approximate the response function around the critical point in our optimal design problem.

4. RESULTS AND DISCUSSIONS

4.1. Effect of Each Design Variable

For the optimization problem considered in [25], the set of optimal design variables is: α=9.82°, t_{u}=0.024, x_{u}=0.667, and x_{l} =0.500. The value of the response function $f(\alpha,\ t_{\mathrm{u}},\ x_{\mathrm{u}},\ x_{\mathrm{l}})$ is 3.312. Use the design variables as the coordinates for a point in the design space. The critical point for the optimal design has the coordinates (9.82°, 0.024, 0.667, 0.500). To analyze the effect of variations in each variable, the first-order Taylor approximation in Eq. (13) is employed. Eight points around the critical one are chosen to determine the first derivatives. For each design variable, two points are selected where the coordinate for that variable is varied by $\pm$1% of its optimal value, while keeping the other coordinates fixed at their optimal values. For example, for α, the two points corresponding to this variable are (9.9182°, 0.024, 0.667, 0.500) and (9.7218°, 0.024, 0.667, 0.500), where 9.9182° and 9.7218° represent 1% and -1% differences from the optimal value of 9.82°, respectively. After calculating the first derivatives, it follows from Eq. (13) that

$$\Delta f \approx -0.063(\alpha - 9.82) + 12.653(t_{\mathrm{u}} - 0.024) - 0.071(x_{\mathrm{u}} - 0.667) + 0.895(x_{\mathrm{l}} - 0.500), \tag{48}$$

where the coefficients of the variations are from the first derivatives.

Figure **6** presents the results when only one design variable varies while the other variables remain constant. The variations for each variable range from -5% to 5% of the optimal value of the variable. Two

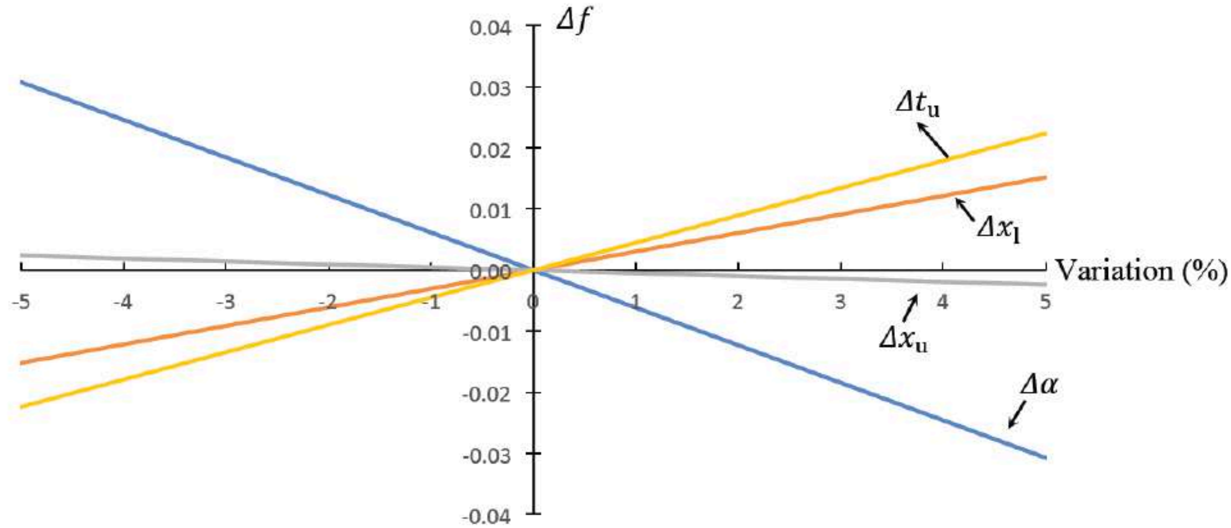

Figure 6: First-order relationships of Δf with $\Delta\alpha$, Δt_{u}, Δx_{u}, and Δx_{l}, respectively. The curve for each relationship is marked with the corresponding variation.

points are observed from this figure. First, for the same percentage of variation, the influence on Δf decreases in the following order: $\Delta\alpha$, Δx_{l}, Δt_{u}, and Δx_{u}. The values of $|\Delta f|$ induced by the first three variations are an order of magnitude higher than that caused by Δx_{u}. For instance, when all variations are 1%, the corresponding values of Δf are -0.0062, 0.0045, 0.0030, and -0.0005, respectively. This suggests that the influence of Δx_{u} is negligible if all design variables are varied by the same degree. Second, small variations in the design variables from their optimal values result in only minor changes to the response function. For example, when $\Delta\alpha$ is -5% or 5%, Δf becomes 0.0307 and -0.0307, respectively, which are approximately 0.9% and -0.9% of the optimal value of *f*, which is 3.312. This indicates that the optimal design is robust. The only concern is whether the variation of a variable causes the set of design variables to fall out of the feasible design space, where all six constraints are satisfied. This issue will be addressed in Sec. 4.3.

In [25], the airfoil shape was approximated using a third-order polynomial function, which depends on t_{u}, x_{u}, and x_{l}. Although the aerodynamic performance of the airfoil is influenced by α, the shape itself is independent of α. Figure **7** shows the airfoil shapes when t_{u}, x_{u}, and x_{l} are varied by 5% from their respective optimal values. These shapes are determined using the polynomial function from [25], by substituting the corresponding values of t_{u}, x_{u}, and x_{l} into this function. As seen in Figure **7**, the varied shapes are nearly identical to the optimal design, confirming that the small changes in the variables result in minimal alterations to the airfoil shape.

4.2. Behavior of the Response Function Around the Critical Point

The behavior of the response function around the critical point is further analyzed using the second-order Taylor approximation in Eq. (38). To determine the first and second derivatives in this equation, 2^4=32 points surrounding the critical point are selected. As with the first-order approximation, for a point related to a specific variable, its coordinate corresponding to that variable is varied by ±1% of the optimal value of that variable. After calculating the derivatives using the numerically obtained function values at these points, the response function can be approximated using Eq. (38) as:

$$f(\alpha,t_u,x_u,x_l) \approx 3.312 - 0.063(\alpha - 9.82) + 12.653(t_u - 0.024) - 0.071(x_u - 0.067) + 0.895(x_l - 0.5) + 0.5[-1.140(\alpha - 9.82)^2 - 189754(t_u - 0.024)^2 - 250(x_u - 0.067)^2 - 466(x_l - 0.5)^2 - 4.401(\alpha - 9.82)(t_u - 0.024) + 0.072(\alpha - 9.82)(x_u - 0.067) - 0.544(\alpha - 9.82)(x_l - 0.5) - 26(t_u - 0.024)(x_u - 0.067) - 42(t_u - 0.024)(x_l - 0.5) - 0.328(x_u - 0.067)(x_l - 0.5)]. \quad (49)$$

Figure **8** shows the relationships of the response function with the variations of the four design variables, respectively. More information can be observed from these non-linear relationships. For example, when the variation of each design variable exceeds 1% or falls below -1%, the new function value becomes lower than the designed value, with the difference increasing as the magnitude of the variation grows. Additionally, it is clear from this figure that $\Delta\alpha$, Δx_{l}, and Δt_{u} have a much greater impact on Δf compared to Δx_{u}. However, slight changes in each variable still lead to only minor changes in the function value. When the variations of

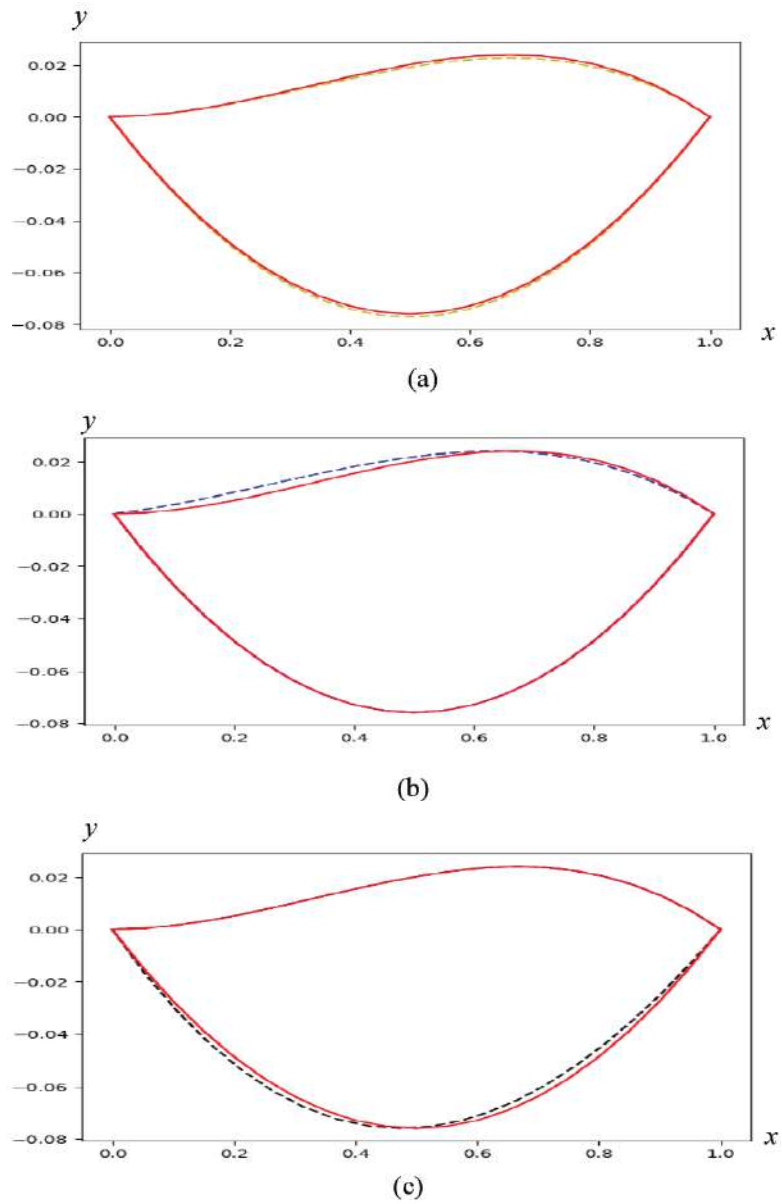

Figure 7: Comparison of the airfoil shapes for 5% changes of (a) t_{u}, (b) x_{u}, and (c) x_{l}, respectively (not to scale). The optimally designed shape is plotted with solid lines, while the varied shapes with dotted lines.

the design variables range -5% to 5%, the largest change in the function value is -0.1682, which occurs when α varies by 5%, as marked in Figure **8**. It is -5.1% of the function's optimal value. This result indicates that small variations in the four design variables leads to only minor changes in the function value, which is consistent with the findings from the first-order model.

The response function depends on four variables. However, as its graph can only be plotted in a 3D space at most, we focus on visualizing the relationship between the response function and the two most influential variables, α and x_l. By setting the terms related to the other two variables to zero, it follows from Eq. (49) that

$$f(\alpha, t_u, x_u, x_l) \approx 3.312 - 0.063(\alpha - 9.82) + 0.895(x_l - 0.5) + 0.5[-1.140(\alpha - 9.82)^2 - 466(x_l - 0.5)^2 - 0.544(\alpha - 9.82)(x_l - 0.5)]. \quad (50)$$

Figure **9** presents the graph of the response function as α varies from 9.4° to 10.2° and x_l changes from 0.46 to 0.54. As observed from this figure, the optimal datapoint, where α=9.82°, x_l=0.5 and *f*=3.312, lies near the peak of the response surface, which reaches a height of 3.314. This observation has three important implications: (i) the maximum value of the response function obtained is not a local maximum for the entire design space, (ii) it represents the maximum value within the feasible design space that satisfies the six constraints, and (iii) the critical point for the optimal

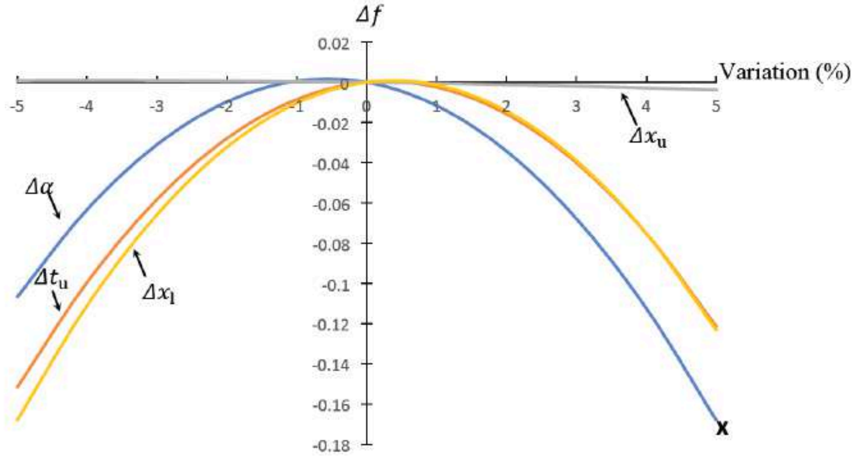

Figure 8: Second-order relationships of Δf with $\Delta\alpha$, Δt_u, Δx_u, and Δx_l, respectively. The curve for each relationship is marked with the corresponding variation. The mark "**X**" denotes the location where Δf has the largest change in terms of magnitude.

design is positioned at the boundary between feasible and infeasible design regions.

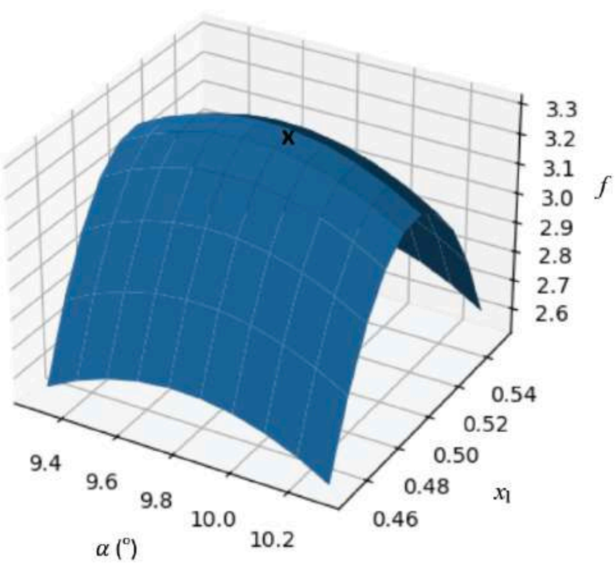

Figure 9: Relationship of the response function with α and x_l around the critical point. The mark "**X**" denotes the location of the optimal design.

4.3. Feasible Design Space Around the Critical Point

In practice, when design variables vary, it is crucial to determine whether the altered design variables still belong to the feasible design space. To do this, the mathematical expression of the feasible design space around the critical point is needed. However, since this expression is unknown in our case, we can instead rely on numerical data to approximate it. One approach is to plot the numerical data to visualize the region they occupy. If a design point lies within this region, it is considered feasible.

Since there are four design variables in our case, their feasible design region is four- dimensional and cannot be directly plotted in a 3D pace. To address this, we propose an alternative method. After obtaining a set of feasible design points around the critical point using an exhaustive search method [25,27], we plot the values of two design variables at a time in a 2D rectangular coordinate system. This approach results in six 2D plots, representing the six combinations of design variables (Figure **10**). Whether a design point belongs to the feasible design space is then determined by examining if it lies within the region covered by feasible points on each of the plots.

Let's consider two cases. In the first case, α decreases by 1% from its optimal value of 9.82°, and x_l decreased by 4% from its optimal value of 0.5. The corresponding design point, p_1, has the values α=9.70°, t_u=0.024, x_u=0.667, and x_l =0.48. The six combinations of two variables are: (9.70°, 0.024), (9.70°, 0.667), (9.70°, 0.48), (0.024, 0.667), (0.024, 0.48), and (0.667, 0.48), which are plotted on the six 2D coordinate systems in Figure **10**. As p_1 lies within the region covered by feasible points in each graph, this design is feasible.

In the second case, α still decreases by 1%, but x_l decreases by 4%, resulting in a design point p_2, with α=9.70°, t_u=0.024, x_u=0.667, and x_l =0.52. The six combinations are: (9.70°, 0.024), (9.70°, 0.667), (9.70°, 0.52), (0.024, 0.667), (0.024, 0.52), and (0.667, 0.52). As seen from Figure **10**, p_2 is located out of three feasible design regions (Figures **10c**, **10e**, and **10f**). Therefore, p_2 is not a feasible design point, which suggests that small variations in the design variables may lead to an infeasible design. In this case, the lift coefficient is calculated to be 0.299, which is below the

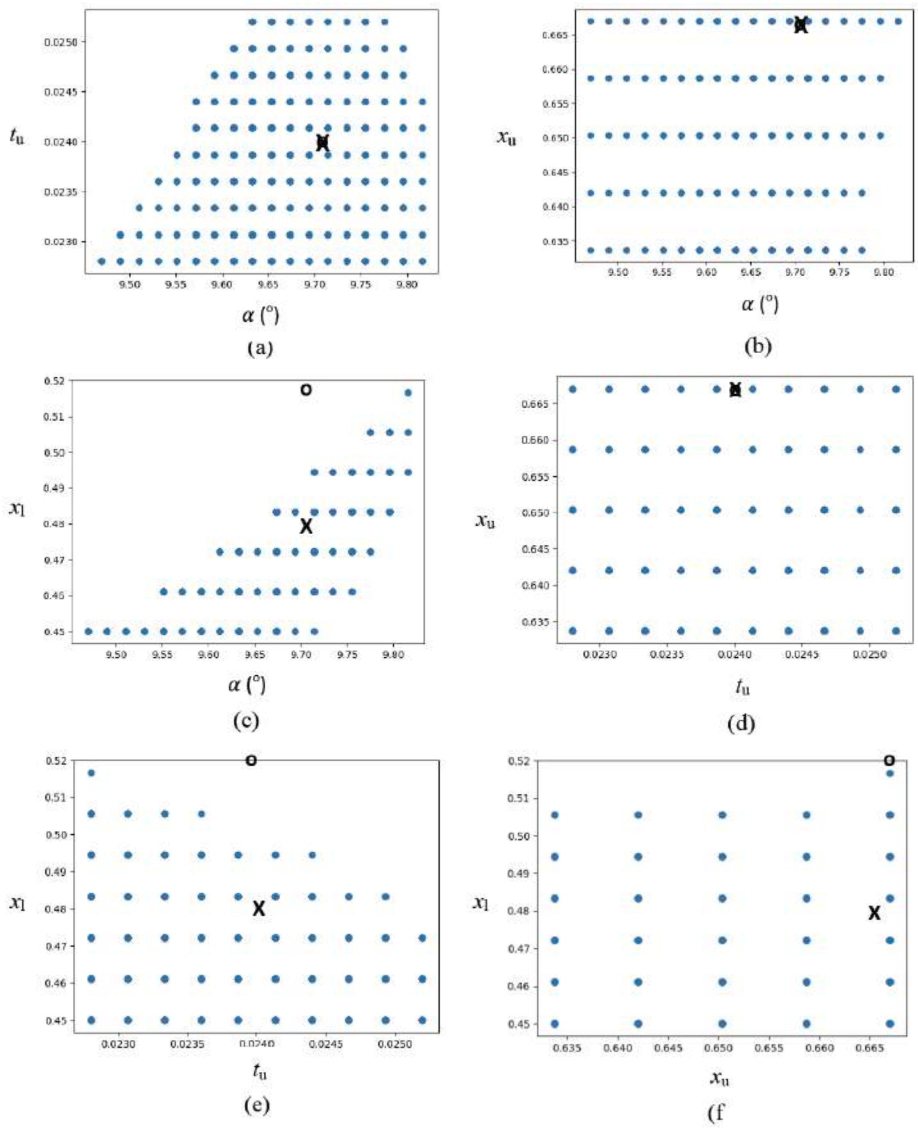

Figure 10: The feasible regions for the combinations of (**a**) α and t_u, (**b**) α and x_u, (**c**) α and x_l, (**d**) t_u and x_u, (**e**) t_u and x_l, and (**f**) x_u and x_l. The feasible region refers to the area covered by the circular dots. The mark "**X**" denotes the location of p_1, and "**o**" the location of p_2. The two marks coincide in (**a**), (**b**) and (**d**).

minimum required value of 0.3. As a result, the aircraft generates less upward force, making it challenging to maintain altitude.

5. SUMMARY AND CONCLUSIONS

In this work, sensitivity analysis was performed by obtaining the first- and second-order approximations of a function using Taylor expansion and finite-difference methods. It was demonstrated that the commonly used factorial design for sensitivity analysis could be explained through these approximations. Using these first- and second-order models, the effects of small variations in the four design variables on the response function were compared. As all these effects were found to be small, the performance of the optimally designed airfoil would not be significantly impacted by minor errors in the design values, such as those that might arise from manufacturing processes. However, it was also found that certain variations could render the design infeasible. Acceptable variations were identified by plotting the feasible design space and verifying whether the resulting design points fall within it.

The sensitivity analysis strategy developed here can be applied to similar engineering design problems. This approach is particularly valuable when the explicit form of the response function is unknown, as it does not depend on an explicit expression and only requires a limited number of data points, which can be obtained through experiments or simulations. This makes it especially useful for problems like those mentioned in

Section 1, such as the design of aerodynamic off-takes [3-6] and ducts [6]. In the future, the method presented in this study will be applied to 3D aircraft geometry design, integrated with advanced computational fluid dynamics analysis.

REFERENCES

[1] Mason RL, Gunst RF, Hess JL. Statistical Design and Analysis of Experiments With Applications to Engineering and Science. John Wiley & Sons, Inc, New York 2003. https://doi.org/10.1002/0471458503

[2] Myers RH, Montgomery DC, Anderson-Cook CM. Surface Methodology: Process and Product Optimization Using Designed Experiments third edition, John Wiley & Sons, Inc. 2009.

[3] Jirasek A. Design of Vortex Generator Flow Control in Inlets. Journal of Aircraft 2006; 43: 1886-1892. https://doi.org/10.2514/1.21364

[4] Hamstra JW, Miller DN, Truax PP, Anderson BA, Wendt BJ. Active inlet flow control technology demonstration. The Aeronautical Journal 2000; 104: 473-479. https://doi.org/10.1017/S0001924000091971

[5] Yurko I, Bondarenko G. A New Approach to Designing the S-Shaped Annular Duct for Industrial Centrifugal Compressor. Int J Rotating Mach 2014; 2014: 925368. https://doi.org/10.1155/2014/925368

[6] Spanelis A, Walker AD. A Multi-Objective Factorial Design Methodology for Aerodynamic Off-Takes and Ducts. Aerospace 2022; 9: 130. https://doi.org/10.3390/aerospace9030130

[7] Thakur V, Kumar R, Kumar R, Singh R, Kumar V. Hybrid additive manufacturing of highly sustainable Polylactic acid - Carbon Fiber-Polylactic acid sandwiched composite structures: Optimization and machine learning. Journal of Thermoplastic Composite Materials 2024; 37(2): 466-492. https://doi.org/10.1177/08927057231180186

[8] Hasanzadeh R. A New Polymeric Hybrid Auxetic Structure Additively Manufactured by Fused Filament Fabrication 3D Printing: Machine Learning-Based Energy Absorption Prediction and Optimization. Polymers 2024; 16(24): 3565. https://doi.org/10.3390/polym16243565

[9] Frank Y, Kenneth M. Ronald Aylmer Fisher. Biographical Memoirs of Fellows of the Royal Society 1963; 9: 91-120. https://doi.org/10.1098/rsbm.1963.0006

[10] Fisher R. The Arrangement of Field Experiments. Journal of the Ministry of Agriculture of Great Britain 1926; 3: 503-513.

[11] Box GEP, Draper NR. Empirical Model Building and Response Surfaces, Wiley, New York, NY, 1987.

[12] Montgomery DC. Design and Analysis of Experiments, eighth edition, John Wiley & Sons, Inc, New York. International Student Version 2012.

[13] Gopalarathnam A, McAvoy C. Effect of airfoil characteristics and trim considerations on aircraft performance, 19th AIAA Applied Aerodynamics Conference (Anaheim, CA, U.S.A.) 2001. https://doi.org/10.2514/6.2001-2409

[14] Gopalarathnam A, McAvoy CW. Effect of airfoil characteristics on aircraft performance, Journal of Aircraft 2002; 39(3): 427-433. https://doi.org/10.2514/2.2968

[15] Letko W, Brewer JD. Effect of Airfoil Profile of Symmetrical Sections on the Low-Speed Rolling Derivatives of 45° Sweptback-Wing Models of Aspect Ratio 2.61, National Advisory Committee for Aeronautics. Washington, D.C., 1949.

[16] Wood RM, Miller DS. Impact of airfoil profile on the supersonic aerodynamics of delta wings. Journal of Aircraft 1986; 23(9): 695-702. https://doi.org/10.2514/3.45364

[17] Aoki M, Nishimura H, Yamakawa E. Effect of Airfoil on rotational noise of helicopter rotor. Aircraft Symposium, 33 rd, Hiroshima, Japan 1995.

[18] McVeigh MA, McHugh FJ. Influence of tip shape, chord, blade number, and airfoil on advanced rotor performance. Journal of The American Helicopter Society 1984; 29(4), pp. 55-62. https://doi.org/10.4050/JAHS.29.55

[19] Teja NNSK, Teja A, Harsha JS, Ganesh S, Ramana KV. Optimization of micro air vehicle airfoil, International Journal of Research in Engineering and Technology 2016; 5(3): 217-219. https://doi.org/10.15623/ijret.2016.0503043

[20] Zhao L, Yang S. Influence of thickness variation on the flapping performance of symmetric NACA airfoils in plunging motion. Mathematical Problems in Engineering 2010; 19. https://doi.org/10.1155/2010/675462

[21] Ismail KA, Rosolen CV. Effects of the airfoil section, the chord and pitch distributions on the aerodynamic performance of the propeller. Journal of the Brazilian Society of Mechanical Sciences and Engineering 2019; 41(3): 1-19. https://doi.org/10.1007/s40430-019-1618-x

[22] Zhang H, Hu Y, Wang G. The effect of aerofoil camber on cycloidal propellers. Aircraft Engineering and Aerospace Technology 2018; 90(8): 1156-1167. https://doi.org/10.1108/AEAT-08-2016-0128

[23] Zhang S, Li H, Jia W, Xi D. Multi-objective optimization design for airfoils with high lift-to-drag ratio based on geometric feature control. IOP Conf. Series: Earth and Environmental Science 2019; 227: 032014. https://doi.org/10.1088/1755-1315/227/3/032014

[24] Zhang R, Li D, Chang H, Wei X, Wang H. Multi-objective optimization on blade airfoil of vertical axis wind turbine. Physics of Fluids 2024; 36: 085172. https://doi.org/10.1063/5.0220194

[25] Han Z, Luo O, Luo C. Optimal Design of a Biconvex Airfoil for a Supersonic Aircraft Using the Basin-Hopping and Exhaustive Search Methods. Journal of Basic & Applied Sciences 2025; 21: 53-65. https://doi.org/10.29169/1927-5129.2025.21.07

[26] Anderson JD Jr. Fundamentals of Aerodynamics, sixth edition, McGraw-Hill Education New York, NY, 2016.

[27] Bernstein DJ. Understanding brute force. Workshop Record of ECRYPT STVL Workshop in Symmetric Key Encryption. eSTREAM report 2005/036, 2005. https://cr.yp.to/snuffle/bruteforce-20050425.pdf

[28] Wales DJ, Doye JPK. Global Optimization by Basin-Hopping and the Lowest Energy Structures of Lennard-Jones Clusters Containing up to 110 Atoms. The Journal of Physical Chemistry A 1997; 101(28): 5111-5116. https://doi.org/10.1021/jp970984n

[29] Baioletti M, Santucci V, Tomassini M. A performance analysis of Basin hopping compared to established metaheuristics for global optimization. J Glob Optim 2024; 89(3): 803-832. https://doi.org/10.1007/s10898-024-01373-5

[30] Nomura S, C Programming and Numerical Analysis: An Introduction. Morgan & Claypool, 2018. https://doi.org/10.1007/978-3-031-79605-0

Nocedal J, Wright SJ. Numerical Optimization. Springer New York 2006.